RESEARCH ARTICLE | JANUARY 15 2019

QP-EPU105: Operational experience with a quasi-periodic undulator at NSLS II FREE

E. Vescovo ✉; K. Kaznatcheev; N. Bouet; Y. Zhu; M. Idir; M. Musardo; C. Kitegi; O. Chubar

AIP Conf. Proc. 2054, 030004 (2019)
https://doi.org/10.1063/1.5084567

QP-EPU105: operational experience with a quasi-periodic undulator at NSLS II

E. Vescovo[1,a),b)], K. Kaznatcheev[1], N. Bouet[1], Y. Zhu[1], M. Idir[1], M. Musardo[1], C. Kitegi[2] and O. Chubar[1]

[1]*National Synchrotron Light Source II, Brookhaven National Laboratory, Upton, New York 11973, USA*
[2]*Synchrotron SOLEIL, Saint-Aubin, BP48, 91192, GIF-sur YVETTE, France*

[a)]Corresponding author: vescovo@bnl.gov
[b)]URL: http://www.aip.org

Abstract. A quasi periodic elliptical undulator (QP-EPU105) has been recently put in operation at the Electron Spectro Microscopy beamline at NSLS-II. Commissioning results pertaining to its initial characterization are presented. The spectral and angular distributions of the light have been probed and compared with emission calculations based on the measured magnetic field. The light polarization produced in parallel and anti-parallel operation modes is also quantitatively analyzed.

INTRODUCTION

The Electron Spectro Microscopy beamline (ESM) has been recently commissioned at NSLS II and is now in operation. The beamline is dedicated to photoemission microscopy. It serves two end stations: a high-resolution angle-resolved photoemission spectroscopy (μ-ARPES) instrument and a full-field photoelectron microscope (XPEEM).

These techniques are best performed in the UV photon energy range where valence band photoemission cross sections are large, high energy and momentum resolution can be achieved and light momentum can be ignored compared to electron momentum. At low photon energies, however, photoemission spectra suffer from spurious signals deriving from undulator harmonics, not efficiently suppressed by the monochromator. This is particularly problematic for high resolution ARPES where one is often dealing with small signals concentrated on a narrow energy region close to the Fermi level. In these cases, any spurious background severely degrades the quality of the data. Photoemission spectra are also strongly dependent from the relative orientation of light polarization and crystallographic axis of the sample under investigation. It is therefore expedient to be able to control the state of polarization of the light.

All these considerations informed the choice of parameters of the insertion device serving this beamline. Considering the parameters of the NSLS II storage ring [1], an optimal magnetic period is found to be 105 mm. EPU105 covers in first harmonic the energy range 20 to 400 eV.[2] The need of high spectral purity is satisfied adopting a quasi-periodic design of the magnetic structure which induces energy shifts of the undulator harmonics away from exact multiples of the fundamental. Finally control of light polarization is obtained with an Apple II type of device which can be operated in parallel as well as in anti-parallel mode.

Spectral characteristics of QP-EPU105

Magnetic optimization of APPLE-II type Elliptically-Polarizing Undulators (EPU), as well as other insertion devices for the NSLS-II, was done using the Radia 3D magnetostatic computer code [3, 4]. This optimization allowed for selecting the main EPU parameters period and transverse dimensions of magnet blocks to satisfy spectral requirements of a beamline at different polarizations for a given allowed minimal value of the vertical magnetic gap and given remanent magnetization of the magnet material. To make that sure that the photon energy as low as 15 eV is attainable (allowing for 5 eV safety margin with respect to the 20 eV lowest-energy spectral requirement) in the linear

Proceedings of the 13th International Conference on Synchrotron Radiation Instrumentation – SRI2018
AIP Conf. Proc. 2054, 030004-1–030004-8; https://doi.org/10.1063/1.5084567
Published by AIP Publishing. 978-0-7354-1782-3/$30.00

horizontal polarization mode at 16 mm minimal gap at 1.25 T remanent magnetization of NbFeB magnetic material, the required EPU period was found to be 105 mm.

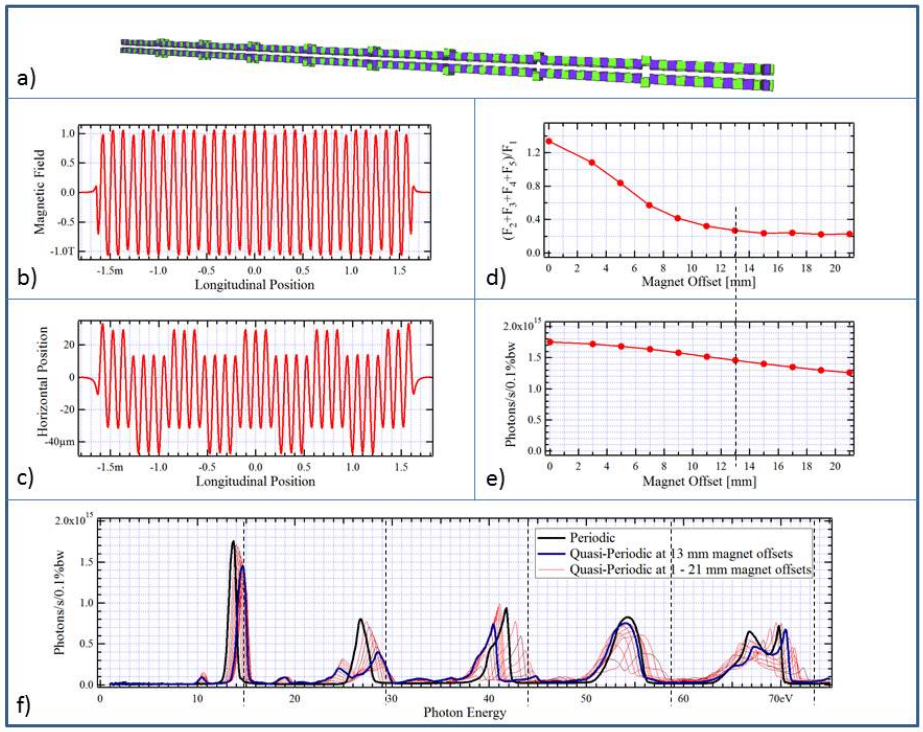

FIGURE 1. Quasi-periodic optimization of the EPU105 (3.4 m version): a) magnet structure with vertically-displaced longitudinally-magnetized blocks at 8 equidistant locations, introducing the quasi-periodic perturbation; b) example of vertical magnetic field in the linear-horizontal radiation polarization mode at minimum (16 mm) gap; c) electron trajectory in the horizontal plane in the magnetic field shown in (b); d) flux ratio at multiples (2 to 5) of the first harmonics photon energy to the peak flux at the first harmonic; e) flux at the first harmonic within 0.6 x 0.6 mrad2 collection aperture vs. vertical displacement of the longitudinally-magnetized blocks; f) spectral flux within 0.6 x 0.6 $mrad^2$ collection aperture for different vertical displacement of the longitudinally-magnetized blocks (vertical dashed lines show spectral locations of the multiples of the first harmonics peak energy).

To increase spectral purity of the radiation transmitted through a grating-based monochromator at low photon energies, quasi-periodic optimization of magnet structure was further performed on this EPU. The goal of this optimization was to shift undulator radiation harmonics, starting from second, off the spectral positions of multiples of the first harmonic peak, and, at the same time, avoid significant flux losses at the fundamental harmonic. This optimization was done using the method based on vertical displacement (towards outside of the horizontal medial plane) of longitudinally-magnetized blocks at several locations of the lower and upper magnet arrays [5, 6]. Such magnet displacement results in a reduction of the field amplitude in one period at the position of the displaced magnet. This does not generate any significant first field integral over the longitudinal position, and allows to easily perform a constrained spectral optimization preserving both the first and second field integrals (at least in the most frequently used linear horizontal polarization mode). To further simplify the quasi-periodic optimization, it was decided to apply same vertical displacement to the longitudinally-magnetized blocks at 8 locations along the structure, separated by equal intervals, as shown in Fig. 1 (a). A typical on-axis magnetic field and the corresponding electron trajectory in the linear horizontal polarization mode after such magnet displacement at the minimal gap of 16 mm are shown in Fig. 1 (b, c). A set of such magnetic fields was calculated for different magnet displacement values using the Radia code, and for each of these fields undulator radiation spectral flux collected through a large (0.6 x 0.6 $mrad^2$) aperture was computed using the SRW code.[7] From each of the computed spectra (see Fig. 1 (f)), the sum of flux values at multiples (2 to 5) of the photon energy corresponding to the peak flux at the first harmonic, was calculated and related to the peak flux at the first harmonic (Fig. 1 (d)). This flux ratio was used as the main criterion of the quasi-periodic

performance. The best magnet displacement value was chosen to be 13 mm, which provides a nearly smallest possible value of the above flux ratio (at the selected parameterization) at no more than 20% reduction of the flux at the first harmonic, see Fig. 1 (e).

We note that in the quasi-periodic magnetic field optimizations of the EPU105, we did not use directly the results published in [8]. Instead, we used a numerical approach, based on a proven high-accuracy computer code [7], that allowed us to optimize the quasi-periodic performance not only for the on-axis single-electron undulator radiation spectral flux per unit surface area, but also taking into account a relatively large flux collection aperture, and finite emittance and energy spread of the electron beam. In our optimizations, we naturally took into account the actual undulator magnet structure with a relatively small total number of periods, the magnetostatics method used to create the required local field perturbations, and we were also able to minimize potential negative impact of these field perturbations on the key characteristics of the undulator magnet structure of importance for the accelerator physics, such as first and second field integrals and their dependence on gap and shift of magnet arrays. A direct application of the theoretical results [8] would not allow us to perform all these constrained optimizations at such a high level of detail. The approach that we applied is not entirely new; elements of it were successfully used in the past for the quasi-periodic optimization of APPLE-II undulators at ELETTRA and at SOLEIL [6].

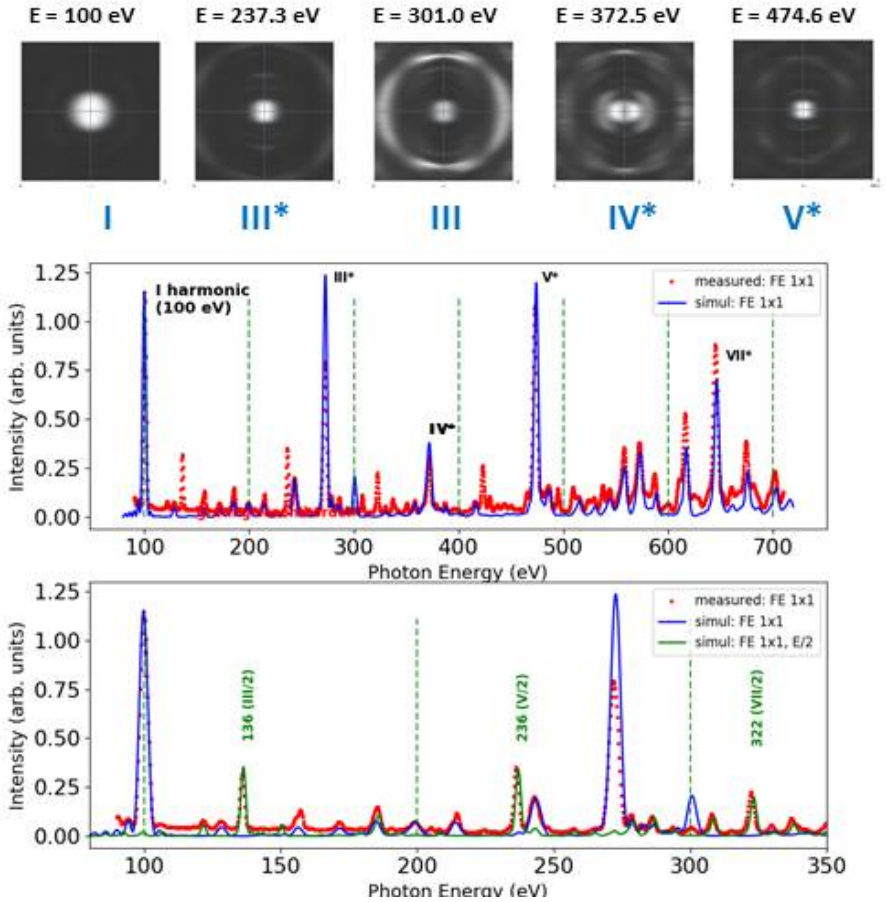

FIGURE 2. QP-EPU105 spectral distribution vs. the monochromator photon energy measured with 1x1 mm^2 front end slits opening. Center panel: measured (red curve) vs. simulated (blue curve) The green dashed lines mark exact multiples of the fundamental. Bottom panel: same as middle panel on a reduced energy range; additionally the calculated curve is rescaled to half its nominal energy (green dots). Top panel: power distributions of QP-EPU105 as seen at the 20 m from the device centre.

In the initial optimizations, the EPU105 was assumed to be 3.4 m long and was expected to be located in a high-beta straight section of NSLS-II. However, at a later stage its length was reduced to 2.8 m to make sure that

it fits, together with a 1.4 m long EPU57 (that is used for higher photon energies, E > 200 eV, at ESM), to a short low-beta straight section of NSLS-II. In this type of straight section, the negative impact of APPLE-II type undulators on electron beam dynamics (reduction of dynamical aperture, lifetime, injection efficiency) is smaller than in the high-beta sections. To fully compensate the impact of APPLE-II undulators on the electron beam dynamics at NSLS-II, special current-strip based feed-forward correction systems were designed to be used on external surfaces of vacuum chambers at the locations of these undulators [9, 10]. This system is particularly important for the EPU105, whose bare impact can be strong even in a low-beta straight section because of its large period. Besides the current-strip system, standard correction coil based feed-forward system is used with APPLE-II (as well as with other insertion devices). One of the main functions of this system in the case of the EPU105 is to compensate relatively large horizontal second field integrals in the linear-vertical and circular polarization modes that are related to the quasi-periodic field modification used in this undulator.

We note that EPU105 was magnetically assembled and shimmed at the NSLS-II insertion device lab [11]. A dedicated genetic algorithm based optimizer computer code [12] was used in these processes.

The spectral distribution curves displayed in Fig. 2 illustrate typical results obtained from QP-EPU105. In this case, the gap is set to 48.2 mm corresponding to a fundamental energy of 100 eV. A calibrated Si photodiode, located downstream the exit slits of the monochromator, is used to provide a signal proportional to the photon flux. Flux vs. photon energy curves are obtained by scanning the monochromator (red dots in Fig. 2).

The effects introduced by the quasi periodicity are immediately noticeable. The flux is suppressed very effectively for energies multiples of the fundamental (green dashed lines). All high intensity harmonics (peaks III*, IV* and V*) are shifted to lower energies with respect to their nominal positions.

The emission spectrum calculated from *first principles*, starting from the measured magnetic field of QP-EPU105, is also shown in Fig. 2 (blue curves). Clearly the agreement with the experimental data is very satisfactory. The position and relative intensities of almost all features are well reproduced. As a matter of fact, the main discrepancies are due to replica of the higher harmonics passing in second order through the grating (peaks at 136, 236 and 322 eV). This can be better appreciated from the bottom panel of Fig. 2 where the experimental data and the calculated spectra are displayed up to 350 eV . In this plot the energy axis of calculated spectrum is rescaled to half its nominal value (green curve). In this way one can see that the peak at 136 eV is actually due to the intense third harmonic (III*) with photon energy 272 eV, passing through the grating in second order (272=136*2). Similarly replicas of the V* and VII* harmonics are also clearly identified.[13]

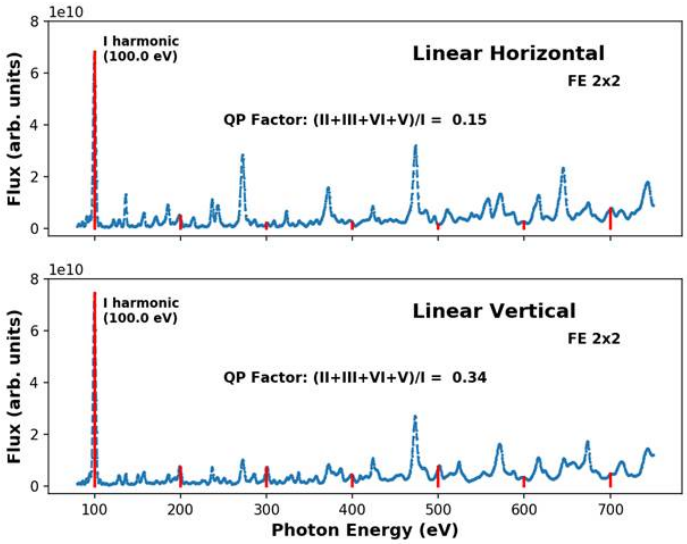

FIGURE 3. QP-EPU105 spectral distribution vs. the monochromator photon energy measured with 2x2 mm^2 front end slits opening. The first harmonic and its multiples are marked in red. Top panel: linear horizontal light (gap=48.2 mm, phase = 0 mm). Bottom pannel: linear vertical light (gap=32.0 mm, phase = 52.5 mm). Note the higher intensity of the first harmonic compared to Fig. 2 resulting from the larger front end slits.

Further insight on the properties of QP-EPU105 can be obtained by examining the angular distribution of the emitted radiation. Angular distributions are obtained by plotting the power distributions on a screen located sufficiently far from the undulator centre (in our case approximately 20 m downstream, corresponding to the location of our front end slits). Plots of this type are shown in the top part Fig. 2. Interestingly the odd harmonics (I, III*, V*), although considerably displaced in energy by the quasi periodicity, still maintain their high brightness. Their power distribution is well described by simple Gaussian profiles. Note that at the exact multiple of the first harmonic (III), the residual radiation is actually highly dispersed away from the centre. This can also help in the pursuit of high spectral purity. This outer radiation can be efficiently stopped by the front end slits, without appreciable loss on the flux of the first harmonic.

Although the QP optimization has been carried out focusing on the performances with linear horizontal light, the QP effect is still present in linear vertical mode (see Fig. 3). In particular the higher harmonics are still effectively displaced toward lower photon energies but the intensities at exact multiples of the first harmonic are somewhat higher in linear vertical compared to linear horizontal light. In other words, a significant decrease of higher order contaminations can be expected also for polarizations other than linear horizontal.

Angular Distribution

The angular distribution of the undulator radiation can be probed with a DiagOn diagnostic. This type of diagnostic has been developed at Soleil.[14] It consists of a multilayer mirror operated in Bragg reflection at 45^o incidence. After reflection the beam is passed through a YAG crystal, whose front face is coated with a semi-transparent Ag film to suppress visible light from the dipole magnets. Images of the YAG crystal are collected by a CCD camera. Our DiagOn is located at 27.2 m from the centre of QP-EPU105.

The parameters of the multilayer are chosen to enhance the reflectivity of the soft x-ray beam at a specific energy. In our case, the multilayer consisted of 150 bilayers of Cr and Sc with a d-spacing of 29.6 angstroms deposited on a 31mm-diameter (111) Silicon substrate with a 5nm Cr underlayer. The deposited thicknesses for Cr and Sc were chosen for optimal reflectance at 45 degrees incidence. The multilayer was deposited in-house [15] by DC magnetron sputtering using 3" diameter targets. Power used was 170W for both materials and target purity was 99.95

Typical DiagOn results for QP-EPU105 are shown in Fig. 4. The reflectivity of the multilayer for 45^0 incidence displays a sharp peak at 236 eV (panel a)). The DiagOn images represent therefore angular distributions of the radiation at 236 eV. As an example of this type of data, in panel b) is displayed the DiagOn image taken with QP-EPU105 set at 66 mm gap. At this gap, the undulator fundamental is located at 250 eV. The radiation at 236 is then far from the undulator peak and is quite divergent, resulting in a ring shaped figure. This is confirmed by the calculated distribution for monochmatic light (236 eV) for QP-EPU105 with gap 66 mm (panel c).

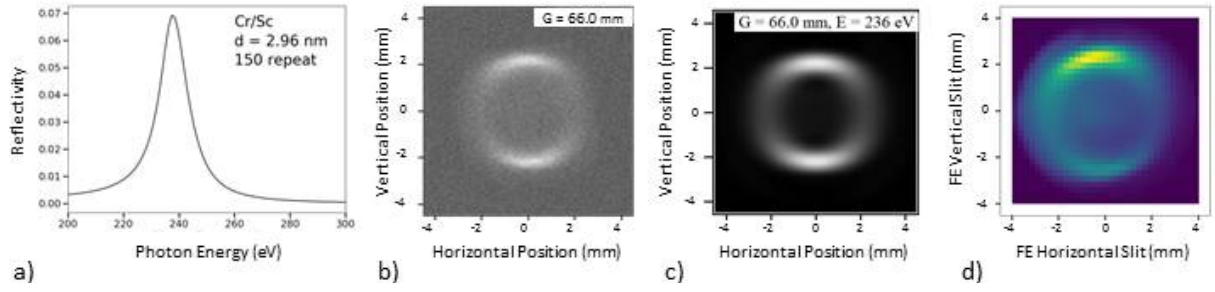

FIGURE 4. a) Calculated reflectivity curve at 45^0 incidence for the DiagOn multilayer. b) DiagOn image from QP-EPU105 set at 66 mm gap in linear horizontal polarization. The image is recorded at 2 mA ring current; c) calculated monochromatic power distribution; d) scanning DiagOn image obtained during regular operation with ring current 320 mA and front end slits aperture of 0.25x0.25 mm.

One of the main advantage of the DiagOn as a diagnostic tool is that its energy filtered images directly reveal the location of the centre of the beam, serving as a powerful beamline alignment tool. For this reason, it is important to be able to collect DiagOn images also during regular operation with high current in the ring. Our multilayer mirrors are mounted on a water-cooled Glidcop holder which allows to operate the device up to approximately 150 mA ring

current. For higher ring currents, however, DiagOn images can still be collected in scanning mode, closing the front end slits to a small, fixed aperture which is then scanned across the beam (see panel d) in Fig. 4). In this way only a small portion of the beam impinges on the multilayer at any given time, allowing to verify the beamline alignment also during regular operation.

Light-Polarization

The EPU105 light polarization properties have been measured using a home-build analyzer located just downstream the monochromator exit slits. Compared to a conventional soft x-ray polarimeter[16], capable of measuring the complete set of Poincare- Stokes parameters, our version is somewhat simplified. It retains only the analyzer part, consisting of a multilayer at fixed incident angle (45^0), a detector (Si diode or YAG screen) and axial (360^0) rotational stages (see left panel in Fig. 5). The lack of the phase retardation portion of a proper polarimeter naturally poses some limitations on the accuracy. We deem this acceptable, as the goal of our instruments is to calibrate the performances of our EPU rather than a comprehensive study of light polarization. Furthermore it can be argued that the symmetric motions of the magnetic arrays in an EPU as well as the necessity to reduce its impact on the electron beam, are all factors that tend to reduce any circular to linear polarization light ad-mixture, bringing the characterization of the EPU light polarization close to the accuracy of our polarimeter.[17]

The analyzer multilayer consist of 100 WSi_2/Si bilayers with a d-spacing of 38.4 angstroms deposited on a 2mm thick (100) Silicon substrate with a 5nm Cr underlayer. The reflectivity measurements performed at first (E=232eV) and third harmonic (E=700eV) confirm sharp WiSi-Si interfaces ($\sigma < 0.2nm$) and suggest high p-to-s light rejection ($< 10^{-3}$).

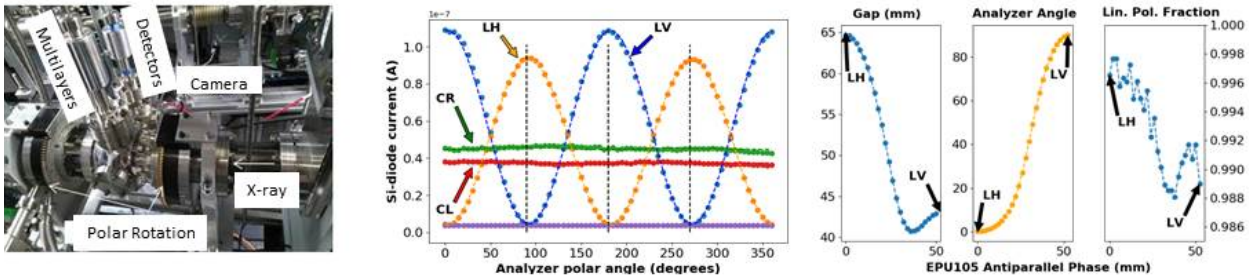

FIGURE 5. Left panel: polarization analyzer. The multilayer and the detectors (Si diode and YAG) are mounted on two translation stages. The entire assembly rotates around the beamline axis. Middle panel: Parallel mode. 45^0 reflectivity curves vs. analyzer polar angle at 232 eV photon energy. Purely linear horizontal (LH) radiation is found at gap = 64.4 mm and phase = 0 mm; purely linear vertical (LV) at gap = 43.25 mm, phase = 52.5 mm; circular left and right (CL,CR) at gap = 49.2 and phase = ± 37 mm. The lines through the experimental points are fits with linear combination of sin and cos functions, used to estimate the degree of polarization. Right panel: Anti-parallel mode. Linear polarized light is obtained for the optimal gap-phase pairs shown on the left; the corresponding inclination of the light polarization is displayed in the middle, while the linear polarization fraction is reported on the right.

The EPU105 mechanical structure consists of two fixed and two diagonally opposed, movable magnetic arrays. To reduce the e-beam disturbance, the array movements are constrained to two operational modes: parallel and anti-parallel. In parallel mode, the diagonally opposed jaws moves in the same direction by the same distance (referred as phase shift). In anti-parallel mode, the mobile, diagonally opposing arrays move in opposite directions by the same amount. The parallel mode of operation produces light with polarization varying between linear horizontal (no phase shift) to circular, to linear vertical (phase shift reaches half EPU period); the anti-parallel mode produces linear polarized light with the polarization plane continuously varying between horizontal (0 mm relative displacement) and vertical (when two jaws are shifted by half of the EPU period in opposite directions).

Results for parallel and anti-parallel modes are shown in Fig. 5, middle and right panel. During these measurements, the monochromator is kept at 232 eV, corresponding to the first harmonic of the multilayer. The intensity of the reflected light is then probed as a function of the analyzer polar angle.

To calibrate the polarimeter axial stage we use EPU with zero phase offset, corresponding to a linear light with polarization vector lying in a horizontal plane. The Si diode intensity variation follows a sinusoidal law with two

distinct maxima of equal height (Fig4, middle panel, orange curve) when x-ray beam is deflected inboard or outboard, inboard position was set to have ninety degree offset. The calibration was further verified by measuring EPU light for girder phase offset equal to half of EPU period (configuration set to produce light polarized in vertical plane). The measured current follows a similar sinusoidal curve, but with maxima at 0^o (beam is deflecting up) and 180^o, as expected. There is a slight variation (10%) of maximum intensity between LH and LV polarizations, which we attribute to misalignment of the polarimeter, finite optimization of EPU gap and some variation of e-beam trajectory, but as the minima of these curves match the background intensity (pink curve; diode current measured with fully open gap), x-ray light has high degree of linear polarization in both cases.

Fitting with a linear combination of sine and cosine functions (dashed lines in Fig. 5) suggest that the degree of linear polarization is 99.8% and 98.9% for horizontal and vertical, respectively. Circular polarized light should show no intensity variation, as the polarimeter rotates around the light propagation direction. Iterative variation of EPU gap and phase helped us to establish such condition (red and green curves). For E=232eV light, CR condition corresponds to 37mm phase shift, CL are generated at -37mm offset. The fitting analysis of these data indicate a degree of circular polarization in excess of 98%.

Results for the anti-parallel mode are shown in the right panel of Fig. 5. To characterize the anti-parallel mode of operation, we first search for optimal gaps at given girder phase shifts (left panel). These gaps correspond to maximum flux at the ML defined energy. Similar to LV and LH curves, the analyzer scans measured for each of these pair of (gap,phase) follow almost pure sinusoidal law with phase intermediate between LV and LH curves. They are fitted to extract polarization inclination angle (middle) and sinusoidal amplitude, taken as a fraction of linear polarized light (right).

The measurements procedure can be repeated for different ML harmonic number (in our case we measure appreciable intensity even at 3-th order of ML reflectivity) or at the energies given by different multilayer. That will provide a set of EPU characterization (girder position for required polarization properties) on a finite energy grid, which can be used to refine the EPU magnetic model. A final look-up table (girder phase and gap position for given energy and polarization) can be generated using SRW simulation. Work in underway to implement this procedure for ESM beamline.

Summary

To conclude, ESM quasi-periodic EPU105 has been commissioned and extensively characterized. It substantially improves the spectral purity of ESM beamline without drastic impact on e-beam or induced complexity for beamline operation. The spectral and angular distribution of the radiation produced by QP-EPU105 are found to be in very good agreement with the calculations used for its design.

ACKNOWLEDGMENTS

This research was performed at the ESM beamline at the National Synchrotron Light Source II, a U.S. Department of Energy (DOE) Office of Science User Facility operated for the DOE Office of Science by Brookhaven National Laboratory under Contract No. DE-SC0012704.

REFERENCES

[1] https://www.bnl.gov/ps/accelerator/

[2] Although not specific to a QP device, generating low photon energies with a medium energy ring (20 eV, 3 GeV NSLSII ring) poses a serious heat load problem, particularly for the first optics. For QP-EPU105 operating at 20 eV, the total power absorbed on M1 is 1.1 kW, assuming 0.4x0.4 $mrad^2$ beam acceptance and 500 mA ring current. This considerable power load is handled by internal water cooling of the M1 mirror. Finite element analysis simulation show that in these conditions, the M1 thermal bump is well simulated by spherical profiles both in the longitudinal and sagittal directions. The maximum slop errors are less than 1 and 6 micro-rad in the longitudinal and sagittal direction, respectively. To reduce heat load on first optical elements, a possibility of EPU105 operation in an elliptical polarization mode, instead of purely linear horizontal polarization mode, is envisaged.

[3] O.Chubar, P.Elleaume and J.Chavanne, A 3D Magnetostatics Computer Code for Insertion Devices, Journal of Synchrotron Radiation, 1998, vol.5, pp.481-484.
[4] O.Chubar, J.Bengtsson, A.Broadbent, Y.Q.Cai, Q.Shen, T.Tanabe, "Parametric Optimization of Undulators for NSLS-II Project Beamlines", SRI-2009, AIP Conference Proceedings Vol. 1234, pp.37-40.
[5] J. Chavanne, P. Elleaume, P. Van Vaerenbergh, Proceedings of EPAC 98, 2213 (1998).
[6] B.Diviacco, R.Bracco, C.Knapic, D.Millo, D.Zangrando, O.Chubar, A.Dael, M.Massal, Z.Marti, Design, construction and field characterization of a variable polarization undulator for SOLEIL, Proc. of PAC-2005, pp.1227-1229.
[7] O.Chubar and P.Elleaume, Accurate and Efficient Computation of Synchrotron Radiation in the Near Field Region, Proc. of the 6th European Particle Accelerator Conference EPAC-98, pp.1177-1179.
[8] S. Sasaki, New Scheme of Quasi-Periodic Undulators, Proc. of IPAC-2010, pp.3141-3143.
[9] J. Bahrdt et al. Active Shimming of the Dynamic Multipoles of the BESSY UE112 APPLE Undulator, Proceedings of EPAC08, WEPC097 p. 2222.
[10] J.Bengtsson, O.Chubar, C.Kitegi, T.Tanabe, "Control of Nonlinear Dynamics by Active and Passive Methods for the NSLS-II Insertion Devices", Proc. of IPAC2012, MOPPP088, pp.759-761.
[11] C.Kitegi, P.Cappadoro, O.Chubar, T.Corwin, H.Fernandes, D.Harder, D.Hidas, M.Musardo, W.Licciardi, J.Rank, C.Rhein, T.Tanabe, Magnetic Optimization of Long EPUs at NSLS-II, Proc. of NAPAC2016, WEPOB57, pp.1018-1020.
[12] O.Rudenko and O.Chubar, An Evolutionary Approach to Shimming Undulator Magnets for Synchrotron Radiation Sources, Lecture Notes in Computer Science, Proc. of 9th Int. Conf. on Parallel Problem Solving from Nature PPSN-IX, 2006, pp.362-371.
[13] The small 300 eV peak present in the calculated spectrum of Fig. 2 is probably real but is suppressed in the experimental data due to carbon contamination of the optics surfaces.
[14] K. Desjardins et al., 2008 IEEE Nuclear Science Symposium Conference Record, Dresden, Germany, 2571 (2008)
[15] R. Conley et al., AIP Conference Proceedings 1365, 69 (2011); doi: 10.1063/1.3625306
[16] H. Wang et al., RSI 82, 123301 (2011), doi: 10.1063/1.3665928
[17] H. Wang et al., J. Sunchrotron Rad. (2012) 19, 944-948, doi: 10.1107/S0909049512034851